

LETTER • **OPEN ACCESS**

Exploring trends in wet-season precipitation and drought indices in wet, humid and dry regions

To cite this article: Chris Funk *et al* 2019 *Environ. Res. Lett.* **14** 115002

View the [article online](#) for updates and enhancements.

Environmental Research Letters



LETTER

Exploring trends in wet-season precipitation and drought indices in wet, humid and dry regions

OPEN ACCESS

RECEIVED

29 April 2019

REVISED

30 September 2019

ACCEPTED FOR PUBLICATION

2 October 2019

PUBLISHED

29 October 2019

Chris Funk^{1,2,5}, Laura Harrison², Lisa Alexander³, Pete Peterson², Ali Behrangi⁴ and Greg Husak²¹ US Geological Survey Earth Resources Observation and Science Center, United States of America² UC Santa Barbara Climate Hazards Center, United States of America³ Climate Change Research Centre and ARC Centre of Excellence for Climate Extremes, UNSW Sydney, Australia⁴ Department of Hydrology and Atmospheric Sciences, University of Arizona, United States of America⁵ Author to whom any correspondence should be addressed.E-mail: chrisfunk@ucsb.edu

Original content from this work may be used under the terms of the [Creative Commons Attribution 3.0 licence](#).

Any further distribution of this work must maintain attribution to the author(s) and the title of the work, journal citation and DOI.

**Keywords:** precipitation, precipitation extremes, climate change, drought, evapotranspiration, global warming, satellite precipitationSupplementary material for this article is available [online](#)**Abstract**

This study examines wet season droughts using eight products from the Frequent Rainfall Observations on GridS database. The study begins by evaluating wet season precipitation totals and wet day counts at seasonal and decadal time scales. While we find a high level of agreement among the products at a seasonal time scale, evaluations of 10 year variability indicate substantial non-stationary inter-product differences that make the assessment of low-frequency changes difficult, especially in data-sparse regions. Some products, however, appear more reliable than others on decadal time scales. Global time series of dry, middle, and wet region standardized precipitation index time series indicate little coherent change. There is substantial coherence in year-to-year variations in these time series for the better-performing products, likely indicative of skill for monitoring variations at large spatial scales. During the wet season, the data do not appear to indicate widespread global changes in precipitation, reference evapotranspiration (RefET) or Standardized Precipitation Evapotranspiration Index (SPEI) values. These data also do not indicate a global shift towards increasing aridity. Focusing on SPEI values for dry regions during droughts, however, we find modest increases in RefET and decreases in SPEI when wet season precipitation is below normal. Dry region SPEI values during droughts have decreased by -0.2 since the 1990s. The cause of these RefET increases is unclear, and more detailed analysis will be needed to confirm these results. For wet regions, however, the majority of products appear to indicate increases in wet season precipitation, although many products perform poorly in these regions due to limited observation networks, and estimated increases vary substantially. *Synopsis:* Our analysis indicates a lack of increasing aridity at global scales, issues associated with non-stationary systematic errors, and concerns associated with increases in reference evapotranspiration in global dry regions during droughts.

1. Introduction

While droughts typically involve a lack of available water, they are complex, slow onset disasters that vary by social and/or environmental context. Despite advances in rapid economic and technological progress, every continent remains exposed to the negative impacts of severe drought. In general, disasters have continued to take a large economic and humanitarian toll between 1998 and 2017; climate-related disasters resulted in nearly \$2.3 trillion dollars (USD) in

damages—a 68% percent increase over the previous 20 year period (UNISDR/CRED 2018). In particular, droughts have contributed to food and price disruptions in many developing countries. Between 1998 and 2017, droughts impacted 1.5 billion people, accounting for one third of all disaster impacts (UNISDR/CRED 2018). According to the Emergency Database (EM-Dat) (EM-Dat 2019), between 2015 and 2018, droughts affected nearly 430 million people, resulting in reported economic losses of \$33 billion dollars (USD). This impact helped fuel a recent increase in

global hunger (FAO, IFAD, WFP, and WHO 2018) and a ~70% increase in extreme food insecurity (Funk *et al* 2019).

As global temperatures increase, the influence of this warming on precipitation and droughts remains a topic of great concern. One clear influence relates to increases in atmospheric saturation vapor pressures (SVP). By definition, SVP is a measure of the amount of water vapor that the atmosphere can hold at 100% relative humidity (i.e. at saturation). SVP increases non-linearly with increasing temperature. So, a warmer atmosphere can, in theory, hold more water, and this effect, described by the Clausius–Clapeyron relations, indicates a ~7% increase in the SVP for every degree of warming. As atmospheric moisture content increases, precipitation will also likely increase (Trenberth *et al* 2003). At a global scale, however, there must be a balance between top-of-the-atmosphere radiative cooling and the latent heating of the atmosphere by condensation/precipitation (Allen and Ingram 2002, Pendergrass and Hartmann 2014). Thus, global increases in precipitation seem to be on the order of 2%–3% per degree of warming. Precipitation extremes, however, are not limited by this large-scale constraint, and are likely increasing (as explored elsewhere in this special issue). The impact of these increases, however, may vary by region (Donat *et al* 2016); in dry regions precipitation increases may be offset by evaporation, while in wet areas increased atmospheric moisture convergence can amplify the effects of heavy rainfall (Held and Soden 2006).

If precipitation extremes increase more rapidly than mean precipitation, it could imply an increase in dry days. From first principles, we might expect wetter very wet days interspersed with more frequent dry days. But heavier precipitation events might also mean more runoff generation (and/or soil moisture recharge), so this does not necessarily translate to less water availability even if dry days increase. In practice, the complex factors driving daily seasonal and decadal variations in weather make such variations hard to detect and attribute. Another key factor for droughts is the extent to which warming-induced higher SVP directly affects surface evapotranspiration (ET). ET changes are complicated, as they are modulated by both the physical climate and the vegetation response to increased carbon dioxide and the near-surface vapor pressure deficit (VPD). VPD, the gradient (difference) between SVP and the actual near-surface vapor pressure, can strongly modulate evaporation from the land surface and the release of water vapor into the atmosphere through plant stomata (transpiration). In cases when the amount of available moisture remains constant but temperature increases, higher SVP can produce larger VPD. This effect will probably not cause droughts, but it may make them more intense when they do occur (Trenberth *et al* 2014).

Given that droughts affect billions of people, result in tens of billions of dollars in losses (UNISDR/

CRED 2018), and have helped increase the number of hungry (FAO, IFAD, WFP, and WHO 2018) and food insecure people (Funk *et al* 2019), an evaluation of global drought trends and precipitation data sets can help inform disaster risk management and drought early warning. Unfortunately, for many developing nations, gauge-based precipitation data sets have insufficient coverage, and the number of available stations has declined substantially since the early 1980s. For example, outside of the United States, Brazil, Australia, Mexico and Colombia, the number of stations has declined from around 7200 to near 3200. Africa has seen a decline from around 2400 to 500 (ignoring the Republic of South Africa). South America has seen a decline from ~2500 to ~1000 stations. These problematic declines are exacerbated by poor spatial distributions of stations, both between and within countries. In practice, this severe limitation in station data means that monitoring droughts and drought trends in data-sparse regions requires the use of either satellite-enhanced precipitation estimates or climate model-based reanalyses. Our objective in this paper is to use a new meta-archive of precipitation products (described below) to examine global precipitation trends and the level of agreement and disagreement among eight different data sets.

2. Data

The precipitation data used in this study are from the Frequent Rainfall Observations on GridS (FROGS) database, which contains (quasi-) global data sets of daily precipitation on a $1^\circ \times 1^\circ$ resolution (Roca *et al* 2019). A common quasi-global domain is analyzed (50°S – 50°N) over a common 1983–2016 time period. Please see Roca *et al* (2019) for data set details and references. Since our focus here is on drought, data sets with shorter periods of record were not used. Two of the station-only data sets in FROGS were analyzed: the Global Precipitation Climatology Center’s Full Data Daily (GPCC FDD V2018) and the Climate Prediction Center version 1 (CPCv1). Other data sets (e.g. REGEN) were available but these two represented the most commonly used in current analyses. The REGEN and GPCC share similar gridding techniques and a large amount of common data. This study uses two satellite-gauge products: the Climate Hazards center Infrared Precipitation with Stations version 2 (CHIRPS2.0) and the Precipitation Estimation from Remotely Sensed Information using Artificial Neural Networks Climatic Data Record (PERSIANN-CDR). Four reanalysis products are examined, version two of the Modern Era Reanalysis (MERRA-2), the ERA-Interim reanalysis (ERAi), JRA-55, and the Climate Forecast System Reanalysis (CFSR). Please refer to Roca *et al* (2019) for details on these data sets. Note also that FROGS contains additional data sets with

shorter periods of record or more limited areal coverage that were not included in this analysis.

We also examine RefET calculated from the MERRA-2 reanalysis by Michael Hobbins¹. This data set was created to support global drought monitoring activities carried out by the Famine Early Warning Systems Network (Funk *et al* 2019). The Hobbins archive is calculated using the American Society of Civil Engineers (ASCE) standardized reference evapotranspiration Penman–Monteith equation (Walter 2000). This formulation is widely used to monitor drought in the United States (Hobbins *et al* 2012) and to estimate the Evaporative Demand Drought Index (Hobbins *et al* 2016, McEvoy *et al* 2016). Daily T_{\max} data from the MERRA-2 is also used in our evaluation. MERRA-2 T_{\max} data were used because we are interested in the covariation of temperature and RefET, and using RefET and T_{\max} from the same reanalysis provides a physically consistent source of information. It should be noted that the 34 year period used here is a quite limited time period for identifying droughts (McKee *et al* 1993). For this reason, we avoid the examination of severe droughts, and focus on relatively frequent events associated with Z-scores of less than -0.7 ; such events should occur 24% of the time.

3. Methods and background

3.1. Methods

In this analysis, we examine a subset of precipitation indices as defined by the Expert Team on Climate Change Detection and Indices, as well as the SPI and SPEI. Of particular interest are precipitation totals during the climatologically wettest three months (91 d) of the year. We refer to these accumulations as Wet Season Totals (WST). We focus on this time period because it tends to be the most important for agriculture and runoff generation. WST-based analyses allow us to describe results for the main precipitation season in each location in a single map. This is a suitable framework for many agricultural-focused applications. The map of main-season dates, based on the Climate Hazards Center precipitation climatology (Funk *et al* 2015a), is available in our previous study (Funk 2015b) and shown in supplemental figure 1(A) (SF1A). We also look at the total of wet days within each wet season (Wet Days). Wet days are those defined as having at least 1 mm of precipitation.

We examine the general level of coherence or deviance between each product's WST and wet day statistics and the eight-product ensemble average. Coherence is based on correlation with ensemble averaged WST and Wet Day statistics. Deviance is measured based on root mean squared (RMS) differences between each product and the ensemble average.

Non-stationary systematic errors can make it difficult to identify low-frequency changes in precipitation characteristics. Temporal averaging may accentuate the

errors associated with non-stationary systematic errors. For example, consider two 1° -degree time series of WST from two products, **a** and **b**. All products will contain some form of systematic and random error. So, an observed time series (vector) of WST will actually contain three terms $\mathbf{a}_{\text{obs}} = \mathbf{a}_{\text{true}} + \text{ERR}_{\mathbf{a},\text{sys}} + \text{ERR}_{\mathbf{a},\text{ran}}$. Similarly, we can decompose $\mathbf{b}_{\text{obs}} = \mathbf{b}_{\text{true}} + \text{ERR}_{\mathbf{b},\text{sys}} + \text{ERR}_{\mathbf{b},\text{ran}}$. Since serial correlation in WST totals are typically close to zero, under the assumptions of the central limit theorem, we can expect the standard deviation of the random error terms to scale with $(1/n^{0.5})$. Hence, in the absence of non-stationary systematic errors, averaging in time should increase the coherence and decrease the deviance of our eight data sets. Hence, we contrast results based on interannual and 10 year averaged data, while examining whether or not these data sets are 'fit to purpose' for detecting low-frequency changes in precipitation.

In addition to WST and Wet Day counts, we also examine SPI and SPEI, accumulated over wet seasons. SPI values are based on conditional gamma distribution fits (Husak *et al* 2007). At each location, a two-parameter (shape and scale) Gamma distribution is fitted to all non-zero WST values. These Gamma distributions are then used to transform the observed WST values into standardized Z-scores with a mean of zero and a standard deviation of one. A similar process is applied to estimate the SPEI, except that the SPEI is based on the difference between the WST precipitation and RefET values for the same time period. The SPEI is based on three parameter (scale, shape, and origin) log-logistic distributions fit to the difference between WST and RefET. Following (Vicente-Serrano *et al* 2010), the log-logistic distributions fit to each grid cell are used to transform the observed WST minus RefET values into standardized anomalies.

Finally, following recent studies examining precipitation changes in dry and wet regions (Donat *et al* 2016), we examine SPI and SPEI variations in dry, wet, and middle regions of the Earth. Thresholds for these regions are set at climatological precipitation values of 2.3 and 5.5 mm per day, breakpoints corresponding to the 33rd and 66th percentile breaks, based on the map of ensemble average WST values. Supplemental figure 1(B), available online at stacks.iop.org/ERL/14/115002/mmedia, shows the regions. Our study next looks at changes in SPEI in dry regions when SPI values are less than -0.7 , i.e. when dry regions are experiencing seasonal droughts. Using empirical data, we examine the hypothesis that these regions may be experiencing increased evaporative demand during seasons with below normal precipitation. We conclude with an examination of changes in dry, middle and wet season precipitation between the first and second half of our period of analysis. Do the data sets examined indicate coherent changes in regional precipitation?

3.2. Background

In general, many assessments of changes in drought frequency, intensity, or duration use either statistical indices, such as the Standardized Precipitation Index (SPI) (McKee *et al* 1993), the Standardized Precipitation Evapotranspiration Index (SPEI) (Vicente-Serrano *et al* 2010), or process-based land surface models. These physical land surface models track precipitation-driven fluxes of moisture into the land surface and estimate extraction via evaporation, transpiration, runoff, and sometimes ground flow or deep infiltration. Some approaches, like the Palmer Drought Severity Index (PDSI) use a simple soil water accounting system, incorporating aspects of both models and statistical indices (Dai 2013).

In general, it is broadly accepted that temperature-based estimates of atmospheric water demand tend to over-estimate anthropogenic increases (Sheffield *et al* 2012, Trenberth *et al* 2014). Simple approaches such as the Thornthwaite (Thornthwaite 1948) or Hargreaves (Hargreaves and Samani 1985) estimation procedures are based solely on temperature. Early studies based on these approaches suggested that global warming would be accompanied by large increases in aridity (Dai 2013). Land surface-based estimates, however, suggested much lower increases in aridity (Sheffield *et al* 2012). Changes in atmospheric water demand are not simply functions of temperature but can also be heavily modified by variations in radiation and near-surface wind speeds. More recent assessments suggest that increasing air temperatures will likely exacerbate droughts, but not produce widespread drying on their own (Trenberth *et al* 2014). New work is also demonstrating that coupled atmosphere-land-ocean model simulations tend to indicate much lower tendencies towards increasing aridity than those found when climate change simulations are analyzed using offline models (Milly and Dunne 2016, Greve *et al* 2017).

In this study we examine ‘drought’ as measured by reductions in main-season precipitation, as well as by differences between supply (precipitation) and atmospheric demand (RefET). The upper limit of the amount of atmospheric water vapor that can be extracted from the land surface is commonly referred to as Potential Evapotranspiration (PET) or Reference ET (Hobbins *et al* 2012). Here, we refer to this term as RefET. The RefET value assumes an infinite supply of water. The RefET used in this study is based on the Penman–Monteith calculation⁶. See Maes *et al* (2019) for a recent review and evaluation of alternative approaches. With no water constraint, the upper limit of ET is primarily a function of net radiation at the surface (Q_n), near-surface wind speed (w_s), and VPD. In mm d^{-1} , $\text{RefET} = 86\,400 \cdot (aQ_n + bF(w_s)\text{VPD})$. $F(w_s)$ estimates the relative influence of changes in wind speed, a is a coefficient based on the slope of VPD with temperature, the latent heat of vaporization and the

psychrometric constant, b is a function of the slope of VPD with temperature and the psychrometric constant. RefET is controlled by a radiation term and a term representing the vertical advection of moisture from the surface. The first term will be primarily controlled by changes in cloud or fog cover. The second term responds to the generation of turbulence by wind and the relative difference between VP and SVP. It is important to understand that there are important complex interactions between soil moisture, VPD, radiation, RefET, temperatures and precipitation (Seneviratne 2010). Clear skies often bring increases in radiation, temperature, VPD and decreases precipitation. More radiation and higher VPD values can increase RefET. These increases in atmospheric water demand can exacerbate soil moisture deficits associated with below normal rainfall, negatively affecting crop yields and forage conditions. It is also important to realize that moisture deficits can act to drive increases in air temperature. The incoming radiation from the atmosphere is offset by the fluxes of energy associated with upwelling longwave radiation, the sensible heat flux, and evapotranspiration. Upwelling radiation and the sensible heat flux are functions of temperature. When evapotranspiration diminishes, surface temperatures typically increase to maintain radiative balance. Atypical extreme temperature increases are often both a symptom and a sign of severe wet-season drought. This study examines briefly the covariability of precipitation and RefET but does not analyze the complicated causal relationships between RefET, temperature, and precipitation.

4. Results

4.1. Exploring WST and Wet day coherence and deviance

We begin by examining the coherence and deviance of our products. In this analysis, we compare each product to the ensemble average, acknowledging from the outset that ‘consensus’ may not necessarily mean ‘correct’. Nonetheless, such evaluations can highlight when and where the products are in good agreement. A detailed product-based evaluation is beyond the scope of this study, and all products will have strengths and weaknesses. For example, while station-only data sets will likely be very accurate in areas with dense gauge networks, there are large regions with poor coverage. So, here we concentrate on the general level of agreement among the products, focusing on the question of whether these products appear generally fit-to-purpose for assessing low-frequency changes in drought or pluvials, the type of changes we might expect to be associated with climate change. Hence, we compare each individual product with the ensemble average.

Globally, there is a high level of coherence between all the WST data sets and the ensemble averages

⁶ <https://esrl.noaa.gov/psd/eddi/globalrefet/>

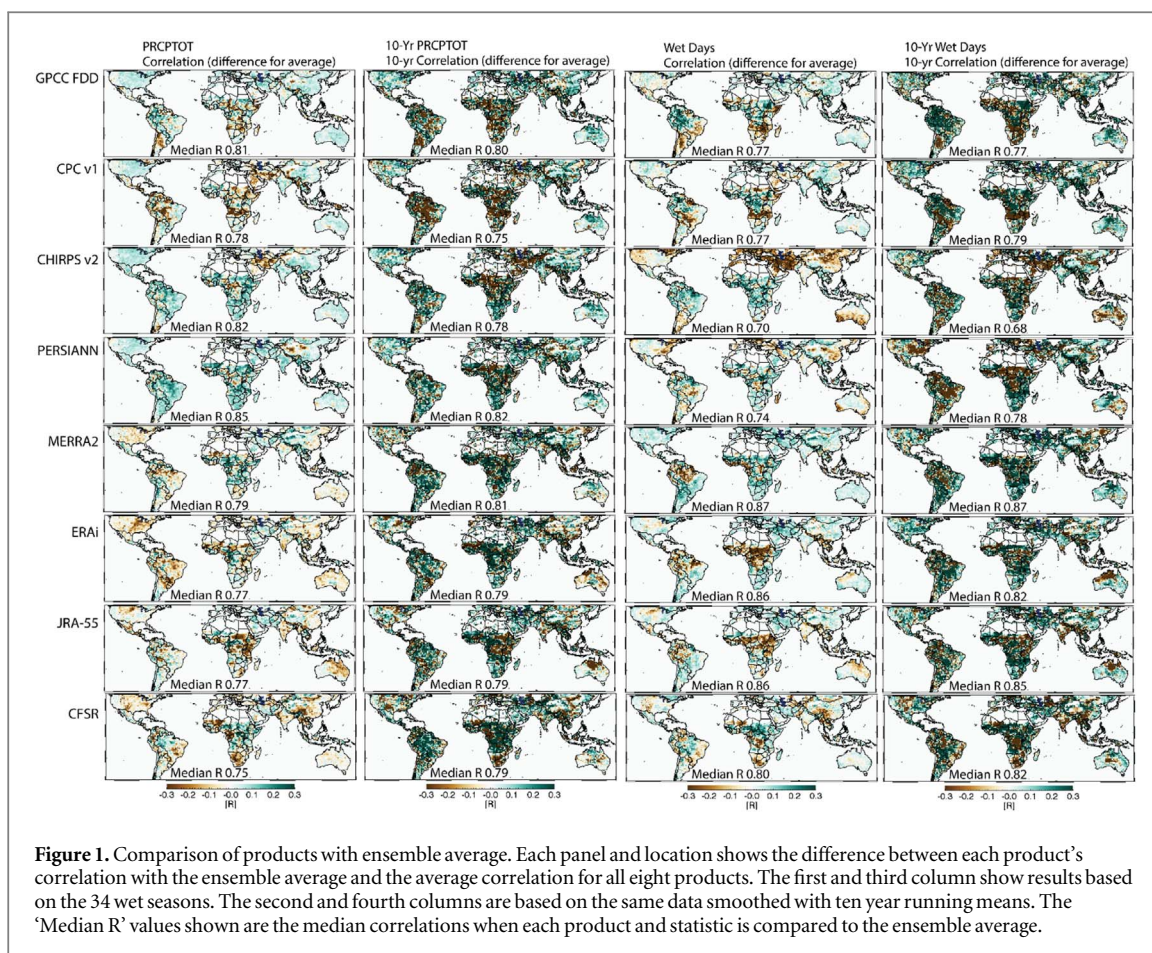


Figure 1. Comparison of products with ensemble average. Each panel and location shows the difference between each product’s correlation with the ensemble average and the average correlation for all eight products. The first and third column show results based on the 34 wet seasons. The second and fourth columns are based on the same data smoothed with ten year running means. The ‘Median R’ values shown are the median correlations when each product and statistic is compared to the ensemble average.

Table 1. Inter-product comparison for Wet Season Totals and Wet Days. Each row presents statistics for an individual product. Correlation and deviance statistics are based on comparison with multi-product average. The ‘annual’ columns present results for standard year-to-year statistics (i.e. all 34 years). The 10 year columns present statistics for the data smoothed with 10 year running means. Deviance is measured based on root mean squared (rms) differences between each product and the ensemble average. The median lag-1 correlation is the median of all lag 1 WST correlations, calculated at each grid cell.

Product	Annual PRCPTOT correlation	Annual PRCPTOT deviance (mm per day)	Median lag-1 autocorrelation	10 year PRCPTOT deviance (mm per day)	Annual wet days correlation	Annual wet days deviance (d)	10 year wet days deviance (d)
GPCC FDD	0.81	0.38	0.03	0.39	0.77	0.5	0.4
CPC v1	0.78	0.38	0.09	0.39	0.77	0.3	0.4
CHIRPS2.0	0.82	0.38	0.03	0.39	0.70	1.0	1.1
PERSIANN	0.85	0.39	0.01	0.43	0.74	0.7	0.7
MERRA2	0.79	0.30	0.06	0.34	0.87	0.4	0.5
ERAi	0.77	0.77	0.10	0.82	0.86	0.3	0.4
JRA-55	0.77	0.43	0.11	0.47	0.86	0.8	0.8
CFSR	0.75	0.43	0.20	0.42	0.80	0.5	0.6

(table 1). We calculated the correlation between each grid’s WST time series and the ensemble average and found the median values of these correlation maps ranged from 0.75 (CFSR) to 0.85 (MERRA-2). Mean deviance values, based on the RMS differences with the mean, ranged from 0.77 mm (ERAi) to 0.3 mm (MERRA-2). The correlation maps for each product were quite similar, so in the first column from the left in figure 1, we show the difference between each product’s correlation map and the average of the eight

correlation maps. These difference maps accentuate the differences between the products. The station-only products perform well in most regions. Data-sparse areas of Africa, South America, Eurasia, and Indonesia appear problematic. The GPCC FDD appears to generally perform better than CPC v1. Satellite-gauge products (PERSIANN and CHIRPS2.0) perform consistently well across most countries, though the CHIRPS2.0 appears to have issues over southwestern Eurasia, near Iran and Turkey. In general, the

performance of the reanalysis products appears lower, with the spatial accuracy patterns varying widely between products. Overall, however, the level of agreement among these products indicates useful levels of skill when assessing year-to-year WST variations across most of the continents.

We next (briefly) explore evidence indicative of non-stationary systematic errors. Median lag-1 autocorrelation values for WST values are close to 0 (table 1), so in the absence of non-stationary systematic errors, averaging should reduce inter-data set differences. Smoothed data have deviance values and median correlation values similar to unsmoothed data (table 1, second column from the left in figure 1). We interpret this as being indicative of substantial non-stationary systematic errors. With a deviance of 0.82, the ERAi stands out as quite problematic. The spatial pattern of relative 10 year correlation strength also varies substantially between products and across regions. In North America, all products appear relatively accurate. In southern Africa, CHIRPS2.0 and PERSIANN may have the highest correlations with the mean at decadal scales. The CPCv1 product has substantially lower correlations over most of Brazil. This may indicate issues associated with poor station density in the CPCv1 product, and the relatively good performance of thermal infrared precipitation estimates in areas associated with deep convective rainfall for the CHIRPS2.0 and PERSIANN. Over Africa, there appear to be substantial disagreements between the products. In general, for South America and Africa, the lack of station data and radiosonde appears to introduce more discrepancies between the WST data sets. Over Eurasia, however, the differences in decadal correlations are substantially lower, except for CHIRPS2.0, which appears to have issues in and around southwestern Eurasia.

Analyses of the coherence and deviance values for Wet Days (right two columns figure 1, table 1) are broadly similar to results for WST values. In general, the product correlations with ensemble averages are quite high, ranging from 0.7 (CHIRPS2.0) to 0.87 (MERRA-2). Spatial maps of differences between the individual and mean correlation maps identify particular regions where each product might have issues. Many countries in southern Africa (Angola, Zambia, Zimbabwe, and Mozambique) have lower correlations in the GPCP and CPC products. CHIRPS2.0 Wet Day correlations are low over western Asia and Europe. MERRA-2 has lower correlations over the west African Guinea Coast and northern Brazil. ERAi and JRA-55 have lower correlations over tropical Africa and South America.

Turning to 10 year running averages of Wet Day time series, we once again find deviance values that are of similar magnitude to the interannual statistics (table 1). We also find relatively large differences in the correlation maps based on the smoothed data (far right column figure 1). Again, we interpret these

results as indicative of relatively large sources of non-stationary systematic differences between the products. These differences affect our ability to identify trends in WST and Wet Day values.

4.2. Examining changes in wet days, SPI, T_{\max} , RefET, and SPEI

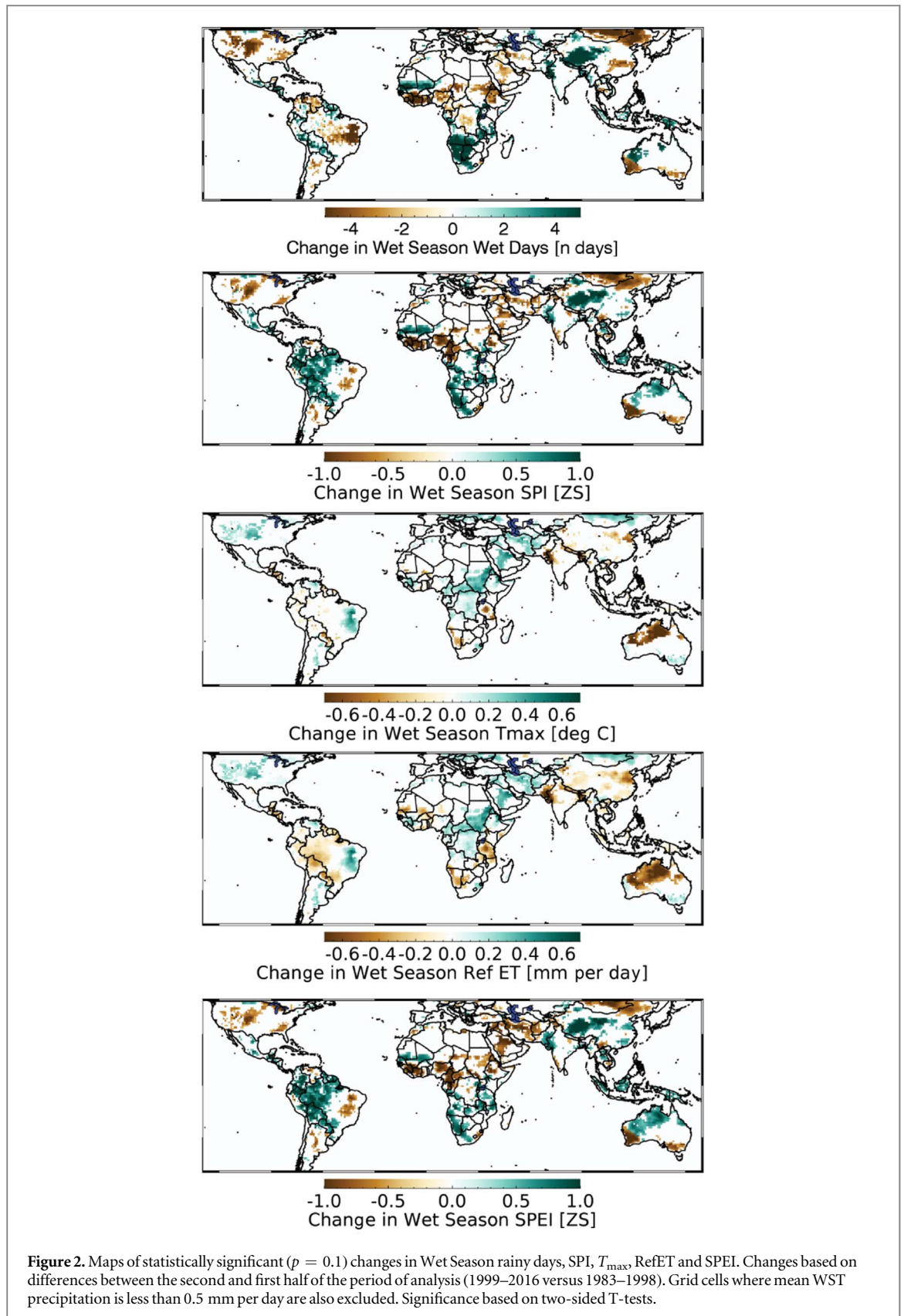
While a detailed examination of long-term changes in drought conditions is beyond the scope of this study, we briefly present changes in Wet Days, SPI, MERRA-2 T_{\max} values, and MERRA-2 RefET. Our Wet Days and SPI trends are based on the ensemble average Wet Days and WST values, respectively. We present these results with the caveat that our results are likely much better constrained in areas with robust observational networks. To explore changes, we present statistically significant differences between the second and first half of our data set (2000–2016 versus 1983–1999). Differences are screened for significance at $p = 0.1$ using a two-sided T-test. Grid cells where mean WST precipitation is less than 0.5 mm per day are also excluded. The wet season appears to be growing shorter and drier over the western Great Plains region of the United States, the Guinea Coast of Africa, Ethiopia, Mongolia, northern China, and Western Australia. The wet season appears significantly longer in Senegal, Burkina Faso, and Mali, western southern Africa, and western China. Increased SPI values are apparent over western South America, Senegal, Burkina Faso, and Mali, western southern Africa, western China, and northern Australia.

Interestingly, changes in MERRA-2 T_{\max} and RefET are quite localized. Many areas that are getting wetter (with increased SPI) have cooled or seen their RefET decrease. RefET decreases in western South America are quite large, and this decrease appears unrelated to changes in T_{\max} , since T_{\max} does not substantially decrease. In northwestern Australia, during the January–March and December–February Wet Season, we find cooler temperatures and large decreases in RefET. The radiation term in the Penman–Monteith formulation tends to be larger than the vertical advection term, and increasing precipitation is likely linked to increases in cloud cover and decreases in RefET in these areas.

While some drying areas (the central-western United States and eastern Brazil) appear associated with increases in T_{\max} and RefET, some areas with significant T_{\max} and RefET increases, like the southwestern United States, do not exhibit significant SPI variations.

The bottom panel of figure 2 combines precipitation and RefET variations by showing changes in SPEI. While overall the pattern of SPI and SPEI are quite similar, there does appear to be increased aridity over the Middle East, Turkey, Iran, and Afghanistan, with SPEI being more negative than SPI.

We should note that figure 2 does not appear to show widespread global increases nor broad decreases



in precipitation, RefET or SPEI. By construction, during the wet season, year-to-year changes in weather, cloud cover, moisture, and temperature advection play a substantial role in modulating local temperature and RefET variations.

4.3. Examining time series of SPI and SPEI for dry, wet, and middle regions

We next examine quasi-global (50°S – 50°N) time series of SPI and SPEI averaged over dry, wet, and middle regions (SF1B). Dry, wet, and middle regions

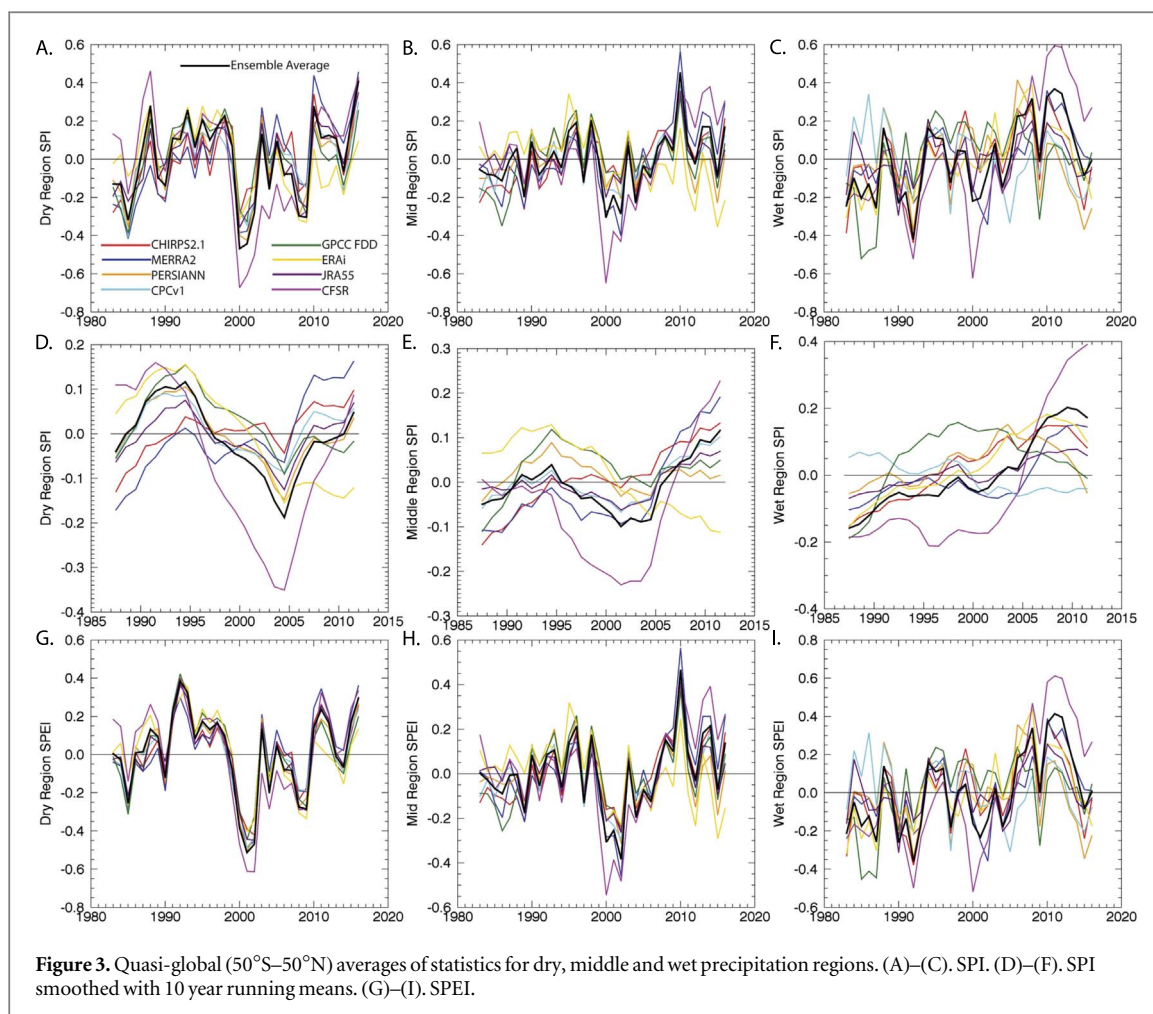


Figure 3. Quasi-global (50°S – 50°N) averages of statistics for dry, middle and wet precipitation regions. (A)–(C). SPI. (D)–(F). SPI smoothed with 10 year running means. (G)–(I). SPEI.

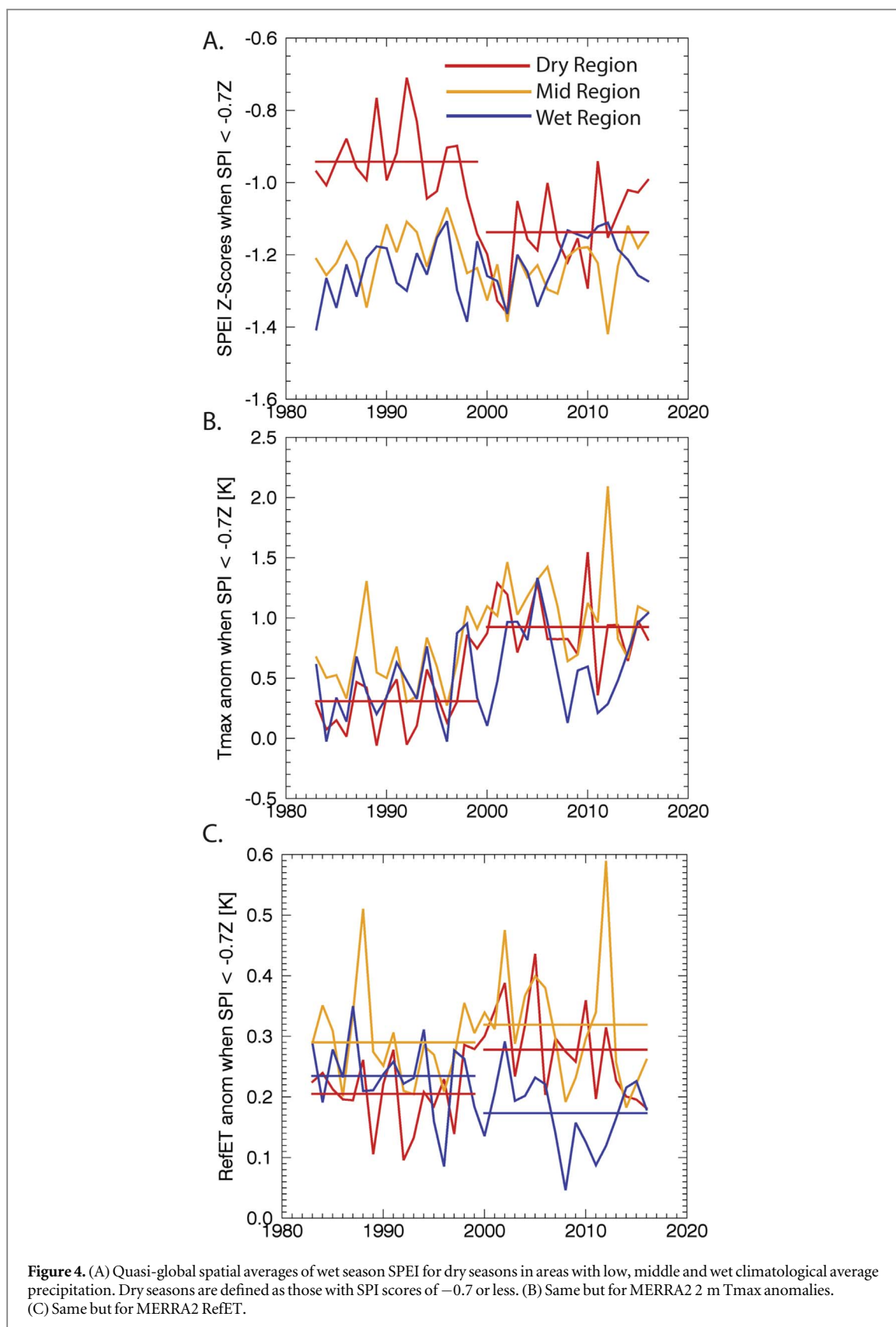
were used in this evaluation because prior research has focused on variations in wet and dry areas (Donat *et al* 2016). We are also interested in the differential role that changes in RefET might play in dryland regimes. Increases in RefET might be enhancing wet season SPEI in these regions. Figure 3(A) shows time series of dryland SPI for each data set, along with the ensemble average. The individual correlations with the ensemble average range from 0.78 (ERAi) to 0.97 (PERSIANN) and the CFSR appears to be associated with the largest decadal excursions. Difference of means tests between the last and first 17 years of data exhibit changes in sign. The two station-only products indicate modest but significant ($p = 0.1$) increases of +0.08 (GPCC) and +0.15 SPI (CPC). The ERAi, which appears to be an outlier, indicates a significant decrease in SPI. The other products indicate non-significant decreases. Overall, this suggests little change, at a global level, in dryland SPI values.

Wet season precipitation in middle-wet regions (figure 3(B)) exhibits broadly similar behavior, although the overall correlation with the ensemble correlations is lower, ranging from 0.42 (ERAi) to 0.92 (CPCv1). Once again, the ERAi appears to be an outlier, exhibiting a significant -0.2 SPI decrease. The other products do not indicate significant declines. Interestingly, in wet regions (figure 3(C)) the

gauge-based CPCv1 exhibits the lowest correlation with the ensemble average (0.45), followed by the gauge-based GPCC (0.53) and gauge-constrained PERSIANN (0.65). This may be due to limited observations in tropical Africa and South America. The year-to-year variations of the CFSR appear unrealistically extreme. Several of the remaining products do appear to exhibit modest significant increases in SPI (CHIRPS2.0 + 0.14, MERRA-2 + 0.08, ERAi + 0.19), but the JRA-55 does not indicate a significant increase.

Plots of 10 year running SPI averages for dry, middle, and wet regions (figures 3(D)–(F)) help accentuate non-stationary systematic differences between the data sets. In all three plots, the CFSR appears to be an outlier. ERAi also appears exceptionally low in the 2000s in dry and middle areas. In wet areas, (figure 3(F)) there are substantial differences between the gauge-only products (CPCv1 and GPCC FDD), both between themselves and the other products.

Examining dry region SPEI (figure 3(G)), we find much higher levels of similarity, because a common MERRA-2 RefET term is now included in each SPEI estimate. This influence is less important in middle regions (figure 3(H)), and even less influential in wet areas (figure 3(I)). The increased spread between the time series shown in figures 3(G)–(I) represents the increasing dominance of precipitation in year-to-year



SPEI variations in more humid regimes. For dryland areas, most of the data sets examined (6 out of 8) indicated significant but small declines in SPEI, ranging from -0.11 to -0.24 SPEI, with the ensemble average change indicating a -0.15 decline in SPEI (significant at $p = 0.03$). Middle regions do not appear to have

substantial SPEI changes. Wet regions, however, do appear to have increasing SPEI values, with all the products except CPCv1 and JRA-55, indicating increases ranging from $+0.04$ to $+0.2$ SPEI.

When viewed through the lens of a SPEI index, these results do appear to broadly support a

Table 2. Analysis of agreement based on regional dry, middle and wet SPI time series. The first column for each Dry/Middle/Wet category presents the 1983–2016 between the individual time series (colored lines in top panels of figure 3) and the multi-product mean (black line in top panels of figure 3). Second column in each set present two-sided T-tests describing the mean change in regional SPI. Values significant at $p = 0.1$ and 0.05 are noted with single* or double asterisks**.

Product	Dry region SPI correlation with ensemble mean	Change SPI, 2000–2016 versus 1983–1999 (Z-score)	Middle region SPI correlation with ensemble mean	Middle region correlation based on 10 year averages	Wet region SPI correlation with ensemble mean	Wet region correlation based on 10 year averages
GPCC FDD	0.89	−0.07Z	0.74	+0.02Z	0.47	+0.09Z*
CPC v1	0.92	−0.01Z	0.92	+0.04Z	0.28	−0.11Z**
CHIRPS2.0	0.83	+0.08Z	0.81	+0.13Z**	0.85	+0.14Z**
PERSIANN	0.97	−0.07Z	0.83	−0.04Z	0.55	+0.03Z
MERRA2	0.81	+0.15Z**	0.90	+0.12Z*	0.85	+0.7Z*
ERAi	0.78	−0.22Z**	0.42	−0.20Z**	0.80	+0.18Z**
JRA-55	0.95	−0.00Z	0.91	+0.00Z	0.75	+0.04Z
CFSR	0.82	−0.08Z	0.78	+0.02Z	0.82	+0.29Z**

perspective in which wetter places are getting wetter, and drier places are getting drier, with the important caveat that substantial inter-product differences remain unresolved. The influence of natural internal climate variations could also play a substantial role in influencing these results.

4.4. Examining SPEI values during droughts for dry, wet, and middle regions

We next focus on potential changes in SPEI during droughts, which we define as wet seasons with SPI values of less than -0.7 . Conceptually, we can partition variations in RefET into those driven by radiation and those driven by vertical advection, with the latter component influenced by wind speed, saturation vapor pressure, and specific humidity (Hobbins *et al* 2012). Warming air temperatures will increase SVP, and it is possible that this influence on RefET may be more apparent during low-rainfall seasons. To explore this hypothesis, we once again calculated SPEI time series over our three rainfall regimes. For this analysis, we used only grid cells with SPI values of less than -0.7 . For consistency, we only carry out this calculation for the MERRA-2 precipitation data set, since the MERRA-2 was also used to estimate RefET. The results are quite compelling (figure 4(A)). For dry areas, we find a highly significant and large -0.2 SPEI decrease between 2000–2016 and 1983–1999. Similar plots of average T_{\max} (figure 4(B)) indicate a substantial $+0.62$ °C warming during droughts over low rainfall regions. While middle-wet areas also exhibit substantial warming, there do not appear to be similar decreases in SPEI, presumably because increasing SVP are offset by other factors. In dry region droughts, there has been an increase in MERRA-2 RefET of $\sim +0.07$ mm per day (figure 4(C)). The increase in RefET for the middle regime is much smaller ($+0.03$ mm per day) and not significant. Interestingly, for wet region droughts, the MERRA-2 RefET actually indicates a substantial and significant decrease of RefET of -0.06 mm per day. This could

indicate the dominance of VPD increases in dry water-limited regimes and increases in cloudiness in radiation-limited wet regimes. It should be noted that increased dryland radiation, perhaps associated with more frequent dry days, might also contribute to increased RefET. Some dry regions have exhibited an observed increase in dry days (figure 2). This could be explored more fully in future work.

4.5. Examining multi-decadal fluctuations in regional SPI

In this section, we return to a main theme of this study, asking whether current precipitation products are adequate to detect large-scale changes in wet season rainfall. To this end, table 2 presents regional correlation and T-test results. The inter-annual correlations for dry, middle and wet regions are reasonably high, likely indicating that current products are generally adequate for monitoring year-to-year variations in wet season rainfall at large regional scales. For dry regions, the ERAi exhibits the lowest correlation ($R = 0.78$). The ERAi also exhibits a weak correlation for middle regions ($r = 0.42$). For wet regions the CPCv1, GPCC FDD, and PERSIANN exhibit poor correlation values of 0.28, 0.47 and 0.55, respectively. While detailed causal analysis is beyond the scope of this study, we conjecture that the poor middle region performance of the ERAi may have to do with non-stationarities within the ERA assimilation system. Because the GPCC data are used to constrain the monthly PERSIANN archive, the three poor-performing wet region data sets are those most strongly constrained by station data, which may be sparse in some wet regions, such as those in central Africa or Amazonia. The variance of dry region CFSR appears higher than all the other data sets (figure 3(A)), and this pattern appears in the middle and wet regions as well (figures 3(B) and (C)).

Table 2 also presents T-test results based on comparisons of 2000–2016 and 1983–1999. For dry and middle regions, there appears to be little evidence for change. The two most significant results (MERRA2 $+0.15Z$ and ERAi

–0.22Z) indicate changes opposite in sign. If there is some change, it appears smaller than the discrepancies between the products. Results for the middle region are broadly similar. For wet regions, however, there does appear to be more agreement among the different data sets. While the least correlated data set (CPCv1) indicates a decline, the other data sets indicate increases, which are significant at $p = 0.05$ for six products: GPCC FDD, CHIRPS2.0, PERSIANN, MERRA2, ERAi, and CFSR.

5. Conclusions and discussion

This study used the FROGS data set to explore potential changes in wet season droughts. While certain products had issues in specific regions, overall, the level of performance at seasonal time scales appears quite good, based on a comparison of the individual products with the multi-product average. For both wet season totals and counts of wet season rainy days, the median correlations for all the products is greater than 0.7, and typically greater than 0.8. All the products appear to perform quite well (figure 1). For climate change detection and attribution analysis, however, accurate assessments at decadal time scales are necessary. This study tested for non-stationary systematic errors in the data sets by utilizing the null hypothesis that in the absence of such errors, inter-product differences should decrease when the data are temporally smoothed. In the absence of non-stationary systematic errors, random inter-data set differences should cancel decreasing inter-product deviance. This decrease was not observed (table 1). While a detailed study is beyond the scope of this analysis, more research into the source of these non-stationary systematic errors may be needed. This research need appears especially important because different types of precipitation data sets have different strengths. In well-gauged areas, station-based data sets will perform very well. Large portions of the Earth, however, remain poorly gauged, and the total surface area of all precipitation gauges covers only half a football field or soccer pitch (Kidd *et al* 2017). Within tropical Africa and South America, data limitations make gauge-only estimates of decadal variations challenging. These regions are also challenging for reanalysis systems. Inhomogeneities in the data streams forcing reanalysis may lead to systematic non-stationary biases.

Consistent with a strengthening of the Walker Circulation (L'Heureux *et al* 2013), and increases in the West Pacific Warming Mode (Funk and Hoell 2015), most significant decadal shifts in wet season precipitation, SPI, and SPEI tend to align with La Niña-like teleconnection patterns (figure 2). Increases are found across much of South America, southern Africa, western China and Nepal, Oceania and northern Australia. The largest decreases appear to be along the Guinea Coast of Africa. Wet season precipitation

changes were analyzed over wet, dry, and middle regions of the globe (figure 3). In general, agreement between products, for the global averages, was substantially better for dry areas versus wet regions. This likely reflects both the heteroscedastic nature of precipitation estimate errors and the challenges of rainfall estimation in poorly instrumented monsoon regions. The difficulty of estimating low-frequency changes is emphasized by plots of 10 year averaged SPI (figures 3(D)–(F)).

Focusing on recent (post-2000) precipitation variations in wet regions (figure 3(C)), we see substantial differences between many of the products. While one might expect that rising temperatures and associated increase in SVP should result in rainfall increases in these wet regimes, inter-product discrepancies make it difficult to authoritatively answer this question, especially because the number of available stations in products like the GPCC and CHIRPS2.0 have declined dramatically in the last 5–10 years (Becker *et al* 2013, Schneider *et al* 2017). Screening the data sets by quality, however, tends to align with increases in mean rainfall. The gauge-only CPCv1 appears to be an outlier in figure 3(C); it correlated poorly with the mean of the other products at decadal scales (figure 2, second column). The CFSR variations in figure 3(C) are extremely large. Several products do appear to exhibit modest significant increases in wet region SPI (table 2), but the large differences between smoothed wet region time series (figure 3(F)) make it difficult to confidently identify increases.

The study also focused on the behavior of SPEI variations during droughts, with droughts defined as wet seasons with SPI values of less than -0.7 . While there is currently a broad consensus on the expectation that increasing evaporative demand will enhance the intensity of droughts (Trenberth *et al* 2014, Behrangi *et al* 2015), our results emphasized the spatial characteristics of the observed changes. Wet and middle region SPEI did not exhibit substantial decreases during droughts, but dry region SPEI has declined by about 0.2 (figure 4(A)). While both dry and middle region T_{\max} exhibit a substantial increase (figure 4(B)), only dry region SPEI decreased. Changes in RefET (figure 4(C)) indicate that dry region RefET increases much more substantially during droughts. The general tendency of RefET in a warming world continues to be a matter of substantial debate and research. It is possible, for example, that increases in cloud cover and aerosols may act to diminish downwelling radiation (Roderick and Farquhar 2002) or reduce transpiration by plants (Swann *et al* 2016, Yang *et al* 2019). Going forward, more detailed process-based analysis of the RefET increases (as implied in figure 4) can help elucidate the potential risks involved in these drought events. Future studies may employ decomposition techniques previously used to analyze United States RefET changes (Hobbins *et al* 2012).

Overall, one of the most interesting aspects of our study is that we do not find widespread changes in precipitation nor increases in RefET or decreases in SPEI. For precipitation, our results may indicate modest increases, in line with expectations associated with radiation limitations (Allen and Ingram 2002, Pendergrass and Hartmann 2014), with larger increases in wet regions potentially associated with enhanced SVP and moisture convergence (Held and Soden 2006). For RefET and SPEI, we see regional areas of increase and decrease (figure 2), but little coherent change on a global scale. Time series of regional SPEI indicate little systematic decrease (figure 3). These results may be consistent with recent modeling studies emphasizing relatively mild anthropogenic increases in aridity (Milly and Dunne 2016, Greve *et al* 2017).

One important conclusion that can be derived from this study is that non-stationary systematic errors provide a major obstacle to analyzing low-frequency changes in the hydrologic system. In the absence of such errors, one would expect the deviations of the smoothed time series to be in much greater accord than on interannual time scales. This was not found to be the case. Station-based archives face limitation from the 21st century ‘Reporting Crisis’ in which the already poor networks of reporting global precipitation gauges continues to degrade. Reanalyses face challenges associated with both modeling precipitation effectively and assimilating coherently changing sets of forcing data. While our examination of eight data sets found high levels of agreement at interannual time scales, more research into the causes of low-frequency disparities will help move hydrologic science forward, while also enhancing our ability to model decadal trends in data-sparse regions of the developing world.

Acknowledgments

This research was supported by the US Geological Survey’s Drivers of Drought program, the USAID Famine Early Warning Systems Network, and the USAID/NASA Harvest program. LA is funded by Australian Research Council grants CE170100023 and DP160103439. We would like to thank the Climate Hazards Center’s scientific editor, Juliet Way-Henthorne, for many helpful suggestions.

Data availability

The data that support the findings of this study are openly available at DOI: <https://doi.org/10.14768/06337394-73A9-407C-9997-0E380DAC5598> (Roca *et al* 2019).

References

- Allen M R and Ingram W J 2002 Constraints on future changes in climate and the hydrologic cycle *Nature* **419** 224
- Becker A, Finger P, Meyer-Christoffer A, Rudolf B, Schamm K, Schneider U and Ziese M 2013 A description of the global land-surface precipitation data products of the Global Precipitation Climatology Centre with sample applications including centennial (trend) analysis from 1901-present *Earth Syst. Sci. Data* **5** 71–99
- Behrangi A, Loikith P, Fetzer E, Nguyen H and Granger S 2015 Utilizing humidity and temperature data to advance monitoring and prediction of meteorological drought *Climate* **3** 999–1017
- Dai A 2013 Increasing drought under global warming in observations and models *Nat. Clim. Change* **3** 52–8
- Donat M G, Lowry A L, Alexander L V, O’Gorman P A and Maher N 2016 More extreme precipitation in the world’s dry and wet regions *Nat. Clim. Change* **6** 508
- EM-Dat 2019 Emergency Database (<https://emdat.be/>)
- FAO, IFAD, WFP, and WHO 2018 The State of Food Security and Nutrition in the World 2017: Building Resilience for Peace and Food Security 9251098883 (<http://fao.org/3/a-i7695e.pdf>)
- Funk C and Hoell A 2015 The leading mode of observed and associated changes in Indo-Pacific climate *J. Clim.* **28** 4309–29
- Funk C, Verdin A, Michaelsen J, Peterson P, Pederos D and Husak G 2015a A global satellite assisted precipitation climatology *Earth Syst. Sci. Data Discuss.* 7 1–13 (<https://earth-syst-sci-data.net/7/275/2015/essd-7-275-2015.pdf>)
- Funk C *et al* 2015b The climate hazards infrared precipitation with stations—a new environmental record for monitoring extremes *Sci. Data* **2** 1–21
- Funk C *et al* 2019 Recognizing the famine early warning systems network (FEWS NET): over 30 years of drought early warning science advances and partnerships promoting global food security *Bull. Am. Meteor. Soc.* **100** 1011–27
- Greve P, Roderick M L and Seneviratne S I 2017 Simulated changes in aridity from the last glacial maximum to 4×CO₂ *Environ. Res. Lett.* **12** 114021
- Hargreaves G H and Samani Z A 1985 Reference crop evapotranspiration from temperature *Appl. Eng. Agric.* **1** 96–9
- Held I M and Soden B J 2006 Robust responses of the hydrological cycle to global warming *J. Clim.* **19** 5686–99
- Hobbins M T, Wood A, McEvoy D J, Huntington J L, Morton C, Anderson M and Hain C 2016 The evaporative demand drought index: I. Linking drought evolution to variations in evaporative demand *J. Hydrometeorol.* **17** 1745–61
- Hobbins M, Wood A, Streubel D and Werner K 2012 What drives the variability of evaporative demand across the conterminous united states? *J. Hydrometeorol.* **13** 1195–214
- Husak G J, Michaelsen J and Funk C 2007 Use of the gamma distribution to represent monthly rainfall in Africa for drought monitoring applications *Int. J. Climatol.* **27** 935–44
- Kidd C, Becker A, Huffman G J, Muller C L, Joe P, Skofronick-Jackson G and Kirschbaum D B 2017 So, how much of the earth’s surface is covered by rain gauges? *Bull. Am. Meteorol. Soc.* **98** 69–78
- L’Heureux M L, Lee S and Lyon B 2013 Recent multidecadal strengthening of the walker circulation across the tropical pacific *Nat. Clim. Change* **3** 571–6
- Maes W, Gentile P, Verhoest N and Gonzalez Miralles D 2019 Potential evaporation at eddy-covariance sites across the globe *Hydrol. Earth Syst. Sci.* **23** 925–48
- McEvoy D J, Huntington J L, Hobbins M T, Wood A, Morton C, Anderson M and Hain C 2016 The evaporative demand drought index: II. CONUS-wide assessment against common drought indicators *J. Hydrometeorol.* **17** 1763–79
- McKee T B, Doesken N J and Kleist J 1993 The relationship of drought frequency and duration to time scales *Proc. 8th Conf. on Applied Climatology (Anaheim, CA)* (Boston, MA:

- American Meteorological Society) 179–83 (http://droughtmanagement.info/literature/AMS_Relationship_Drought_Frequency_Duration_Time_Scales_1993.pdf)
- Milly P C D and Dunne K A 2016 Potential evapotranspiration and continental drying *Nat. Clim. Change* **6** 946
- Pendergrass A G and Hartmann D L 2014 The atmospheric energy constraint on global-mean precipitation change *J. Clim.* **27** 757–68
- Roca R, Alexander L V, Bosilovich M G, Potter G, Bador M, Contractor S, Jucá R and Cloché S 2019 FROGS: a daily $1^\circ \times 1^\circ$ gridded precipitation database of rain gauge, satellite and reanalysis products (<https://earth-syst-sci-data.net/11/1017/2019/essd-11-1017-2019.pdf>)
- Roderick M L and Farquhar G D 2002 The cause of decreased pan evaporation over the past 50 years *Science* **298** 1410–1
- Schneider U, Finger P, Meyer-Christoffer A, Rustemeier E, Ziese M and Becker A 2017 Evaluating the hydrological cycle over land using the newly-corrected precipitation climatology from the global precipitation climatology centre (GPCC) *Atmosphere* **8** 52
- Seneviratne S I *et al* 2010 Investigating soil moisture-climate interactions in a changing climate: a review *Earth Sci. Rev.* **99** 125–61
- Sheffield J, Wood E F and Roderick M L 2012 Little change in global drought over the past 60 years *Nature* **491** 435
- Swann A L S, Hoffman F M, Koven C D and Randerson J T 2016 Plant responses to increasing CO₂ reduce estimates of climate impacts on drought severity *Proc. Natl Acad. Sci.* **113** 10019–24
- Thornthwaite C W 1948 An approach toward a rational classification of climate *Geogr. Rev.* **38** 55–94
- Trenberth K E, Dai A, Rasmussen R M and Parsons D B 2003 The changing character of precipitation *Bull. Am. Meteorol. Soc.* **84** 1205–17
- Trenberth K E, Dai A, van der Schrier G, Jones P D, Barichivich J, Briffa K R and Sheffield J 2014 Global warming and changes in drought *Nat. Clim. Change* **4** 17–22
- UNISDR/CRED 2018 Economic losses, poverty and disasters 1998–2017 (<https://unisdr.org/we/inform/publications/61119>)
- Vicente-Serrano S M, Beguería S and López-Moreno J I 2010 A multiscalar drought index sensitive to global warming: the standardized precipitation evapotranspiration index *J. Clim.* **23** 1696–718
- Walter I A *et al* 2000 ASCE's standardized reference evapotranspiration equation *Watershed Manage. Oper. Manage.* **2000** 1–11
- Yang Y, Roderick M L, Zhang S, McVicar T R and Donohue R J 2019 Hydrologic implications of vegetation response to elevated CO₂ in climate projections *Nat. Clim. Change* **9** 44–8